Interface and Heat-affected Zone Features of Dissimilar Welds between AISI 310 Austenitic Stainless Steel and Inconel 657

H. Naffakh[1], M. Shamanian[2*] and F. Ashrafizadeh[3]
Department of Materials Engineering, Isfahan University of Technology, Isfahan, Iran
Received May 5, 2008; Accepted June 10, 2008

Abstract
The aim of this paper is to characterize welding of AISI 310 austenitic stainless steel to Inconel 657 for use in oil-refining industries. The welds were produced using four types of filler materials; nickel-based alloys designated as Inconel 82, A, 617, and 310 SS. The interfaces and heat-affected zones were characterized by optical and scanning electron microscopy. Interfaces on the two sides of the joints showed unmixed and heat-affected zones, while a partially melted zone was observed in the interdendritic regions of the HAZ in Inconel 657. The microhardness profile from the base metal to the HAZ exhibited high hardness in the case of Inconel 657 as an indication of α-Cr precipitation in the HAZ of all the filler materials investigated and as the occurrence of precipitation hardening. It was concluded that undesirable regions such as UZ, HAZ, and PMZ have the least average size for Inconel 82 and 310 SS weldments among the weld metals studied.

Keywords: AISI 310, Inconel 657, Dissimilar welds, Heat-affected zone, Precipitation.

1- Introduction

One of the most important issues in dissimilar welds is the heat-affected zone (HAZ) since it plays a crucial role in the properties and soundness of the weld. Austenitic alloys such as 310 steel and Inconel 657 (ASTM A560 nickel-chromium-niobium superalloy), which are employed in high temperature corrosive media, are considered to be critical in the heat-affected and interface regions because of their scant capability to diffuse heat from the weld to the base metal [1-3]. On the other hand, subjecting Inconel 657 to high temperatures for sufficient time tends to form an extensive precipitation of α-chromium in the austenitic matrix and gives rise to precipitation hardening. Furthermore, heat concentration at joint edges may cause liquid formation as well as initiation followed by propagation of microfissures in the HAZ [1,4]. Presence of low-melting phases in the heat-affected zone can promote hot cracking in the interdendritic regions. Moreover, there is a high potential for grain growth in the HAZ of 310, which significantly decreases the toughness and strength of the weldments. Appropriate selection of the filler metal and the amount of heat input during the joining process of 310 steel to Inconel 657 prevents the formation of the unmixed zone (UZ), the partially melted zone (PMZ), and the heat-affected zone, thus avoiding such phenomena as liquation cracking, grain growth, precipitation, embrittlement, low strength, and severe boundary migration.

The welding process of 310 SS can be accomplished using the conventional fusion techniques such as shielded metal-arc welding (SMAW), gas tungsten-arc welding (GTAW), and gas metal-arc welding (GMAW). Autogenous welding of 310 SS can be performed with 310 SS filler material. For autogenous joining of Inconel 657, either ENiCr-4 electrode or Inconel 617 filler wire and electrode is recommended.

In oil-refiner tower applications, where temperature reaches 1050°C and the atmosphere is both carburizing and oxidizing, the Inconel 657 is a suitable choice as the heat-flow controlling component (damper) and the support (hangers) [5-7]. The rotating axles, which control the damper motion, are made of 310 SS because they are exposed to a lighter atmosphere and lower temperatures. The fusion welding is the normal process for joining dampers to axles located in the wall tower. Nevertheless, for such dissimilar joints, it seems that the type of proper filler material, its microstructural features, physical and mechanical properties of the weld, and weldability have not been sufficiently investigated and there is rather limited published work on these aspects. This study was conducted to investigate the microstructural features of the interfaces and heat-affected zones in 310 SS to Inconel 657 dissimilar weldments.

2- Experimental work

The nominal compositions of the two alloys, AISI 310 stainless steel and Inconel 657, are presented in Table 1. The 310 stainless steel was hot rolled and quenched in water. To dissolve the precipitates, solution annealing heat treatment was carried out on the sheet

* *Corresponding author:*
Tel:+98- 311-3915737 Fax: +98-311- 3912752
E-mail: shamanian@cc.iut.ac.ir
Address: Dept. of Materials Engineering, Isfahan University of Technology, Isfahan, 84156-83111, Iran

1. MSc.
2. Associate Professor
3. Professor

prior to welding. Inconel 657 was received as a plate in casting condition. Samples, 160×60×12 mm^3 in size, were prepared of both materials. Three filler materials, Inconel 82, Inconel 617, and Inconel A as well as one type of stainless steel filler metal and electrode (310 austenitic stainless steel) were prepared for the purposes of this study (Table 1).

The two separate test plates were welded together using a 75˚V groove with a root opening gap of 2.5 mm and a root face of 1mm. Welding was performed using butt weld and filler wires of 2.5 mm in diameter to deposit the passes. The welding parameters are presented in Table 2. In all the cases where the weld metal was deposited by the GTAW process, the shielding gas was argon. The test plates were clamped and their surfaces were clearly brushed using a stainless steel brush prior to welding and after each pass. The weld temperature was allowed to fall below 150 ºC before the next pass. The welding parameters such as voltage (E), current (I), and speed (V) were simultaneously recorded during welding (Table 2). The welding parameters were adjusted to obtain proper fluidity of the molten pool for all the fillers and coated electrodes. Weldments were cut perpendicular to the weld fusion line and specimens were then prepared by the following standard metallography practice. Marble solution (10gr $CuSO_4$ + 50 mlit HCl + 50mlit H_2O) was used as the chemical etching reagent. The microstructures were examined by employing optical and scanning electron microscopy using conventional techniques. Chemical compositions were also analyzed by an energy dispersive X-ray spectrometer (EDS). Moreover, microhardness measurements were made across the weld metals under a 100 g load, using a Leitz Microhardness tester.

Table 1. Nominal composition of base metals and filler materials (wt.%).

	Base metals		**Filler materials**			
Elements	310 SS	Inconel 657	Inconel 82	Inconel 617	Inconel A	310 SS
C	Max 0.1	Max 0.2	Max 0.1	Max 0.1	Max 0.1	Max 0.1
Si	1	1	0.5	1	1	1
Mn	2	1	3	2	3	2
Fe	Rem.	1	3	5.5	12	Rem.
Cr	26	45	20	25	15	26
Mo	-	-	-	10	1.5	-
Co	-	-	-	10	-	-
Ti	-	-	1	0.6	-	-
Nb	-	1	3	1	2.5	-
Al	-	-	-	1	-	-
Ni	21	Rem.	Rem.	Rem.	Rem.	21
Cu	-	-	0.5	0.5	0.5	0.75

Table 2. The welding parameters.

Filler materials	**Welding process**	**Pass number**	**current (A)**	**voltage (V)**	**Welding speed (mm/s)**	**Heat input (KJ/mm)**	**Total heat input (KJ/mm)**
Inconel 82	GTAW	1	120	12	1	1.44	5.93
	GTAW	2	110	12	1.1	1.2	
	GTAW	3	110	14	0.85	1.81	
	GTAW	4	105	12	0.85	1.48	
Inconel A	GTAW	1	135	12	0.77	2.10	8.94
	SMAW	2	105	26	1.76	1.55	
	SMAW	3	105	24	1.43	1.76	
	SMAW	4	105	24	1.25	2.02	
	SMAW	5	105	24	1.67	1.51	
Inconel 617	GTAW	1	130	12	1.20	1.30	7.19
	SMAW	2	90	24	1.58	1.37	
	SMAW	3	110	24	1.15	2.30	
	SMAW	4	120	24	1.30	2.22	
310 SS	GTAW	1	130	12	1	1.56	6.49
	SMAW	2	100	25	3	.83	
	SMAW	3	110	25	1.88	1.33	
	SMAW	4	110	25	1.76	1.56	
	SMAW	5	110	22	2	1.21	

3- Results and discussion

3- 1- Base metal microstructures

Figure 1a shows the microstructure of 310 austenitic stainless steel that was water quenched after hot rolling. The structure mainly consists of fine and equiaxed grains of austenite with annealing twins. These twins are a result of performing annealing process on the sheet after water quenching. There are no considerable carbides or nitro-carbides of alloying elements in the microstructure. As expected, the solidification mode of 310 austenitic stainless steel is involved in the formation of delta ferrite in the austenite matrix. These ferrite stringers are elongated parallel to the rolling direction.

In addition, Inconel 657 shows a relatively complex microstructure. It is completely dendritic and is composed of columnar and equiaxed dendrites. As can be seen in Figure 1b, interdendritic boundaries have experienced severe segregation, which can be recognized by brighter color from darker dendritic cores. In many studies on Ni-Cr alloys, it has been suggested that the niobium in these alloys has a strong tendency to partition to the liquid. Under these conditions, low-melting terminal solidification products, containing NbC and/or Laves phase may form [8]. Furthermore, Ni-Cr alloys containing niobium are more susceptible to solidification cracking than the niobium-free alloys. They may form a terminal solidification product containing the topologically close-packed (TCP) phases such as sigma, P, or μ (mu), which is less detrimental to weldability than the Nb-rich and Laves phases [8,9].

The secondary phases can be observed in Figure 1b, c, and d within the interdendritic regions; white eutectic phases are the result of liquid transformation to austenite + niobium carbide ($L \rightarrow \gamma + NbC$) by eutectic reaction. Typical SEM micrograph of this structure is shown in Figure 1c. Chemical composition of the alloy contains 1-2 wt.% niobium and 0.1 wt.% carbon. Therefore, the formation of this eutectic structure was expected. The results of EDS analysis were in agreement with microstructure (Figure 2a). In many investigations on nickel-base superalloys, this phase is called the 'Chinese script'[8], which predominantly forms in interdendritic regions. Dark phases, which are enriched in chromium and are located near the γ-NbC structure, are the ferrite phase (Fig. 1c and 2b). This phase has an important role on toughness of the alloy at elevated temperatures.

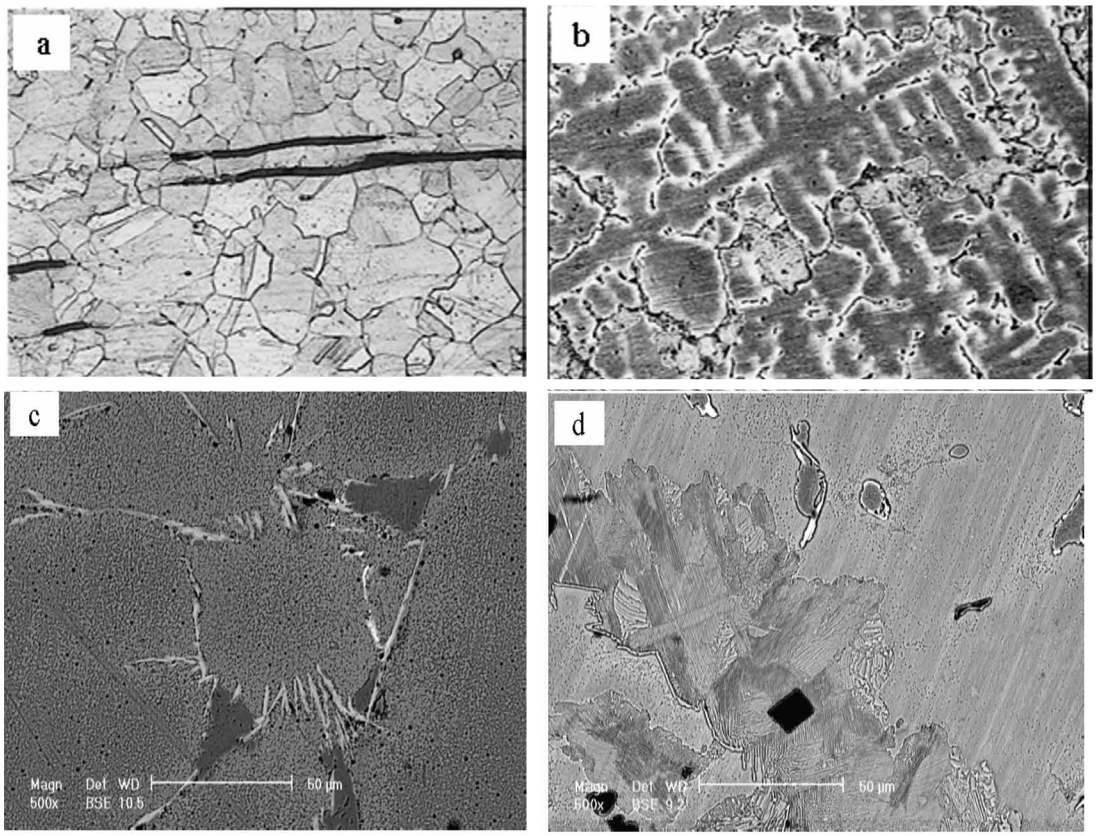

Fig.1 (a) Microstructure of 310 austenitic stainless steel (b) Microstructure of Inconel 657 superalloy (c) White γ/NbC structure and dark ferrite phase (d) Lamellar γ/Laves structure and cubic carbide precipitate.

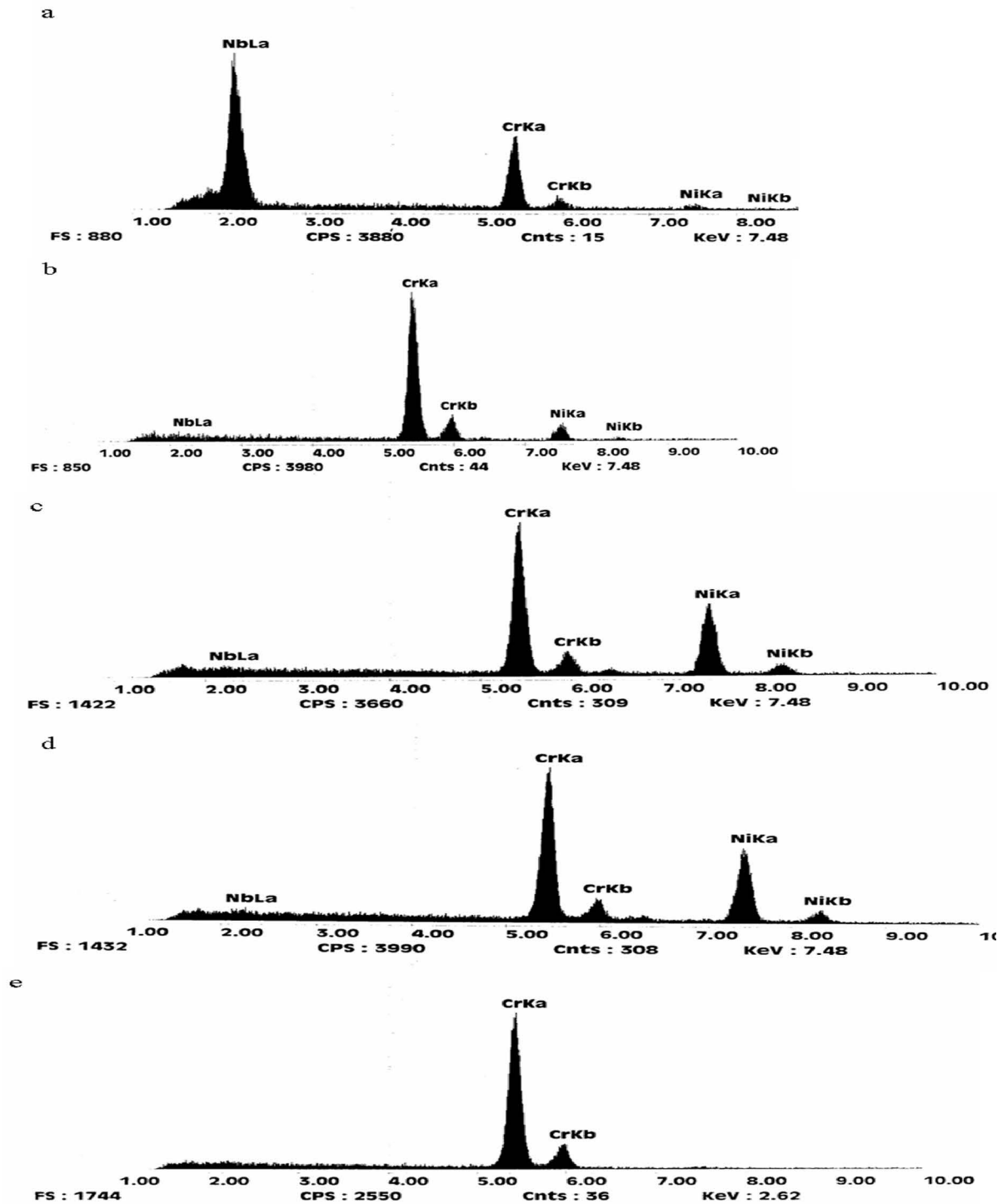

Fig. 2. EDS result for (a) Nb-rich phase (b) Cr-rich phase (c) dark layer of Laves phase (d) bright layer of Laves phase (e) coarse chromium carbide.

In addition, there is another type of eutectic in the alloy microstructure, formed predominantly in the grain boundaries. which seems to be fully lamellar (Figure 1d). This structure can be the result of liquid transformation to austenite + laves (L→ γ + laves) eutectic structure at the last stage of solidification (Fig. 2c and 2d). It is clear that the γ/laves structure has a lower melting point than γ/NbC structure and that, therefore, has an important influence on the solidification cracking of the alloy in the HAZ. Figure 1d displays coarse cubic precipitates; energy dispersive spectroscopy confirmed that these cubic particles were chromium carbides (Figure 2e) produced at the early stages of solidification. Table 3 exhibits chemical composition of secondary phases in Inconel 657 microstructure, extracted from EDS results of Figure 2.

Table 3. EDS results for secondary phases in Inconel 657 microstructure: (a) NbC eutectic (b) α-Cr rich phase (c) Dark layer of Laves eutectic (d) bright layer of Laves eutectic (e) coarse chromium carbide.

	Cr	Ni	Nb
(a)	33.87	5.96	59.78
(b)	76.65	20.94	1.49
(c)	50.10	45.32	1.23
(d)	40.50	54.92	4.58
(e)	96.37	3.63	-

3- 2- Interface and HAZ microstructures

3- 2- 1- Interface and HAZ microstructure in Inconel 82 weld metal

The interface between Inconel 82 weld metal and Inconel 657 base metal is shown in Figure 3a. The unmixed zone appears as a laminar layer, where a small fraction of the base metal has been totally melted and resolidified without undergoing any dilution (Figure 3b). The microstructure of the heat-affected zone (Figure 3a) shows extensive grain boundary melting and liquation. This partially melted zone is characterized by dendritic boundary melting and thickening. The original dendrite boundaries, in many cases, have moved to locations a few microns away. The tendency of boundaries in Inconel 657 to melt is attributed to their niobium enrichment; niobium at these boundaries not only lowers the melting point constitutionally, but also forms low-melting carbide-austenite eutectics during solidification. The base metal microstructure of the Inconel 657 consists of coarse elongated dendrites due to casting process. It may be so considered that the side and tip of dendrites were rounded due to liquation in the HAZ of Inconel 657 and close to the fusion boundary. The partially melted zone in this side of the joint appears to be much wider, compared to the 310 alloy side (Figure 3c), which is the zone of austenite grain coarsening.

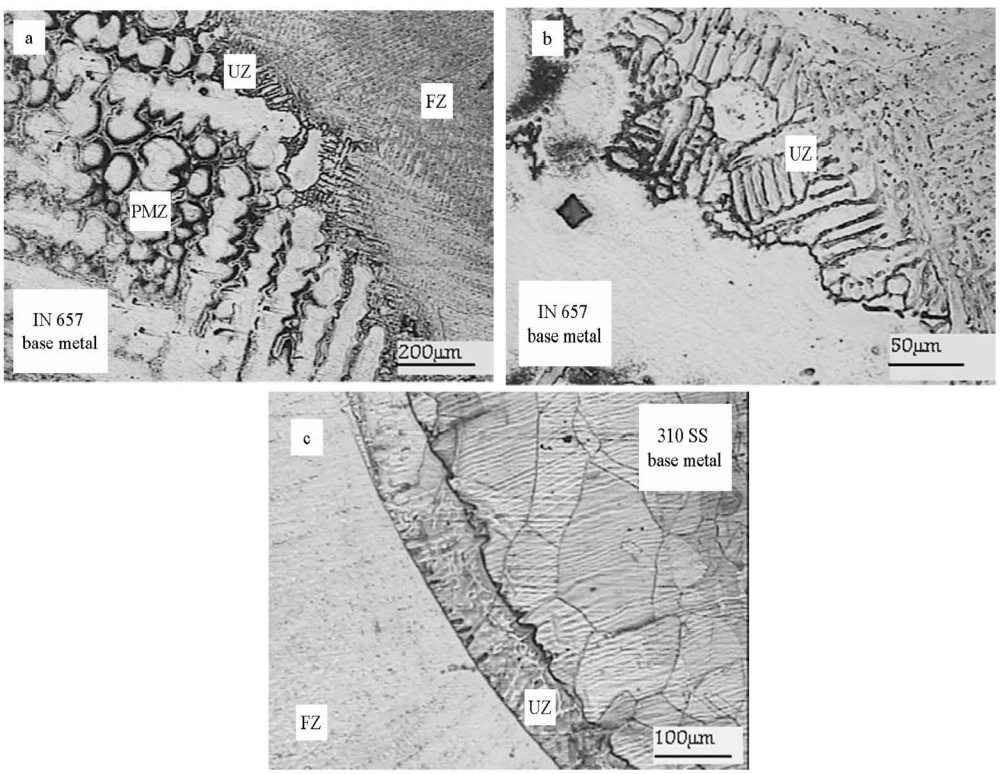

Fig.3. (a) UZ, PMZ, FZ and Inconel 657 base metal related to Inconel 82 weld metal (b) UZ in magnified view (c) UZ, FZ, HAZ and 310 SS base metal.

3- 2- 2- Interface and HAZ microstructure in Inconel A weld metal

The interfaces between Inconel 657 base metal with Inconel A weld metal (Figure 4a) as well as with Inconel 82 weld metal (Figure 3a) show the presence of unmixed zones. A higher magnification of this structure can be seen in Figure 4b. According to Figure 4b, although the UZ size of Inconel A-Inconel 657 interface is wider than UZ size of Inconel A- 310 SS interface, but the average size of the unmixed zone in Inconel A- 310 SS base metal interface (Figure 4c) is wider than that of Inconel 657 side. This might be attributed to the greater compositional differences between the Inconel weld metal (nickel-based) and the 310 SS base metal (iron-based). Welds between dissimilar combinations are known to exhibit wider unmixed zones, where the microstructure and chemical compositions are quite different from the surrounding weld metal [9]. Such large unmixed zones tend to be formed near the interfaces where the base metal has a significantly higher melting point. The melting point of the 310 SS is higher than the Inconel weld metal, and the convection currents are not able to promote adequate fluid flow and mixing. On the other hand, being highly alloyed, Inconel 657 has a closer melting point and composition to the Inconel weld metal. In this case, a wide unmixed zone can not be formed because convection in the weld puddle has caused only a thin laminar layer to remain unmixed.

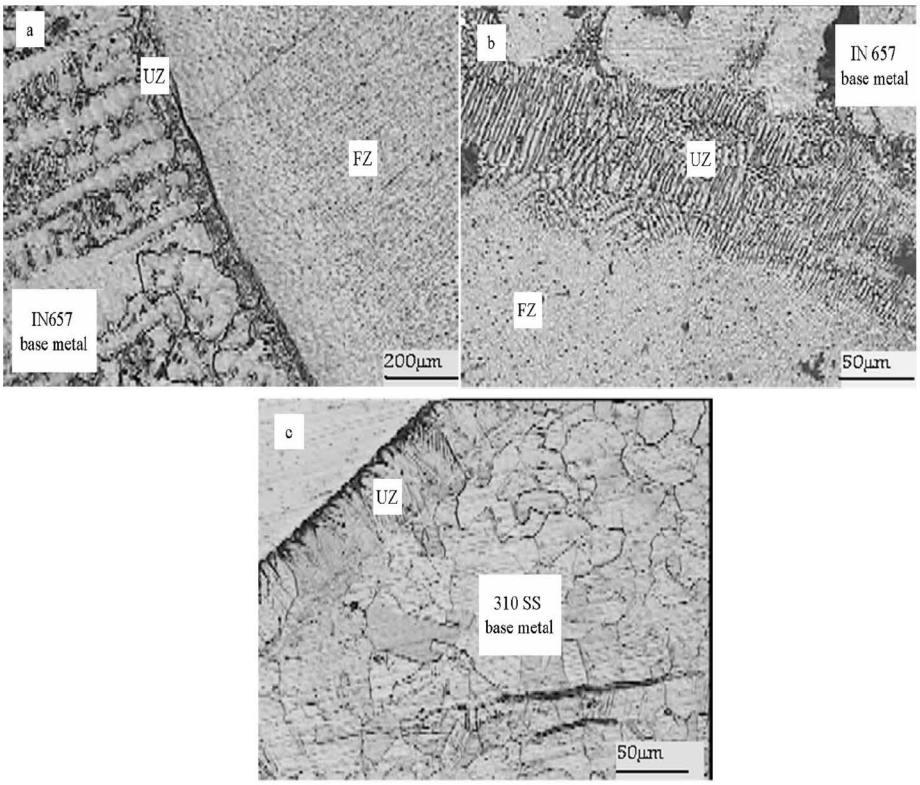

Fig .4. (a) UZ, PMZ FZ and Inconel 657 base metal related to Inconel A weld metal (b) UZ in magnified view (c) UZ, FZ, HAZ and 310 SS base metal.

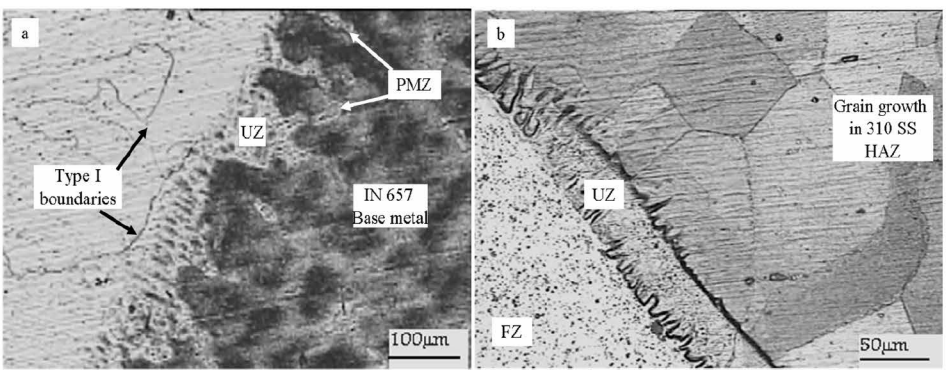

Fig .5. (a) UZ, PMZ, FZ, type I boundaries and Inconel 657 base metal attributed to Inconel 617 weld metal (b) UZ, FZ, HAZ, grain growth and 310 SS base metal.

3- 2- 3- Interface and HAZ microstructure in Inconel 617 weld metal

Figure 5a shows the interface between Inconel 617 weld metal and Inconel 657 base metal with a type I boundary. Type I boundaries are usually observed in homogeneous (similar base and filler metals) welds and are different from grain boundaries in the weld metal of dissimilar welds (designated as type II boundaries). Type II boundaries are just adjacent to the fusion boundary and running parallel to it [9,10]. The former type of welds (epitaxial growth) causes grain boundaries from the base metal substrate to run continuously across the fusion boundary in a direction perpendicular to it. The occurrence of type II boundaries was originally attributed to transition in primary solidification behaviour (from ferritic to austenitic) due to the compositional gradient normal to the fusion boundary. Type II boundary is a result of allotropic transformation in the base metal that occurs on cooling and produces grain boundaries of the type γ:α at the fusion boundary in dissimilar metal (fcc:bcc) welds. It has been shown that type II boundaries can be formed in such dissimilar metal welds only when there is a Ferrite/Austenite phase boundary at elevated temperatures in the base metal. In the present work, all the micrographs, prepared from the interface regions, indicated that only type I boundaries were produced. This was, of course, expected because although dissimilar welds are involved, there is no allotropic transformation during the cooling process for either of the two base metals. On the other hand, severe grain growth occurred in the 310 SS heat-affected zone, which can be seen in Figure 5b.

3- 2- 4- Interface and HAZ microstructure in 310 SS weld metal

Figure 6a and 6b show the interface between 310 SS weld metal and Inconel 657 base metal. At the other side of the joint, the interface between 310 SS weld metal and 310 SS base metal is also shown in Figure 6c. The microstructure reveals the presence of ferrite stringers in some of the austenite grains within the base metal close to the HAZ. These ferrite stringers are probably remnants from the high-temperature primary processing of the base plate. It is clearly known that homogenization of such segregates can not be effective, especially in austenitic alloys. The ferrite stringers have been expanded and grown in width close to the fusion boundary, presumably because more ferrite is usually retained during rapid cooling after the formation of delta ferrite due to the heating cycle. Delta ferrite is also known to be retained in the HAZ grain boundaries of welds, having a composition with a positive ferrite potential. Complete epitaxial grain growth occurred in the case of 310 SS base metal-310 SS weld metal, as shown in Figure 6c.

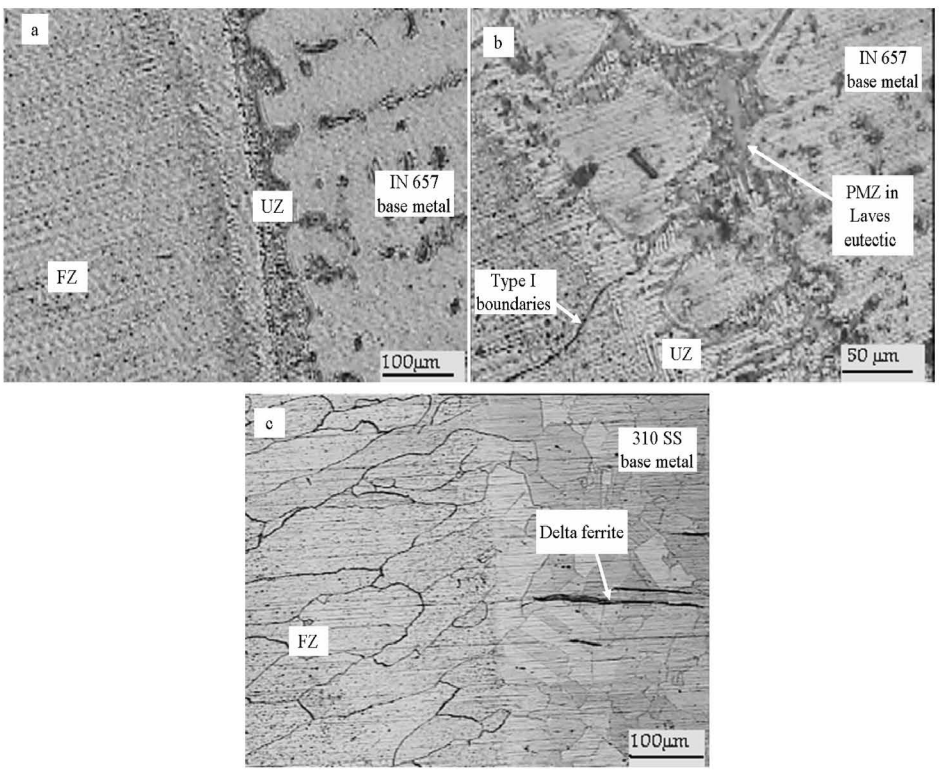

Fig .6. (a) UZ, PMZ, FZ and Inconel 657 base metal related to 310 SS weld metal (b) PMZ in magnified view (c) Delta ferrite, HAZ and 310 SS base metal.

3- 3- Comparison of interfaces and heat-affected zones

Figures 7 and 8 illustrate the average size of the unmixed and the heat-affected zones for the two sides of the joints, respectively. Inconel 657 base metal shows both UZ and PMZ, but no significant PMZ is observed in the 310 SS base metal. This indicates that the 310 SS grain boundaries are depleted from low-melting phases; instead, a severe grain growth has occurred in the HAZ. It is clear that the average heat input to the weld puddle governs the average size and structure of the HAZ and UZ in the two dissimilar base metals [11,12]. In this study, the highest and lowest mean values of the heat input belong to Inconel A and Inconel 617 weld metals, respectively. It is interesting to note that precipitation occurred in the heat-affected zone of Inconel 657. Based on Ni-Cr equilibrium phase diagram, it can be considered that the casting alloy with a composition of 50wt.%Ni-50wt.%Cr has eutectic structure. This lamellar structure consists of γ (nickel-rich) and α (chromium-rich) layers, successively. Inconel 657 casting microstructure mainly consists of an austenitic phase with some small secondary phases enriched in niobium and chromium dispersed in the interdendritic regions. Thus, metallurgically, Inconel 657 base metal has a metastable structure and can be transformed into stable α-Cr precipitates in the austenite matrix if sufficient time and temperature are allowed [1].

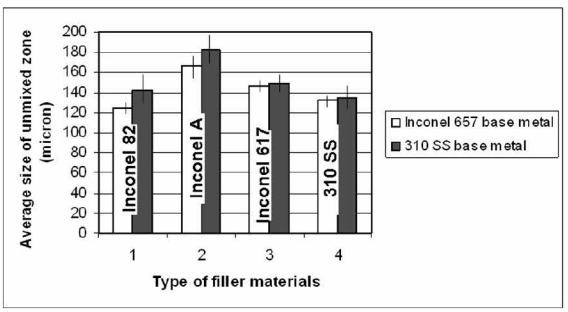

Fig .7. The average size of UZ versus the filler metals type.

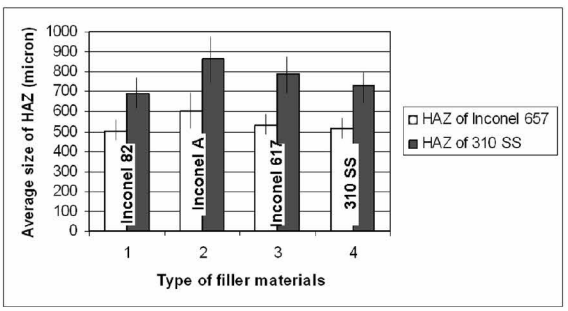

Fig .8. The average size of HAZ versus the filler metals type.

Inconel 657 base metal of all filler materials investigated showed α-Cr precipitates in the heat-affected zone formed in the austenite matrix. Figure 9 displays the precipitation regions of α-Cr precipitates in the HAZ of Inconel 657. It is interesting to note that, in order for the material to have a fully obvious microstructure, it was easier and faster to etch Inconel 657 HAZ than the un-welded Inconel 657 base metal. This indicates that the HAZ of Inconel 657 is more depleted from chromium (the main corrosion resistant element).

Fig .9. Precipitation in Inconel 657 HAZ.

The hardness profile was measured for a more accurate examination of precipitation phenomena in the Inconel 657 HAZ (Figure 10). It can be seen that micro-hardness increases from the base metal to HAZ. Precipitation of chromium-rich phase is the main reason for increasing the hardness. The depletion of chromium can decrease the oxidation resistance and may deteriorate certain mechanical properties such as toughness at elevated temperatures.

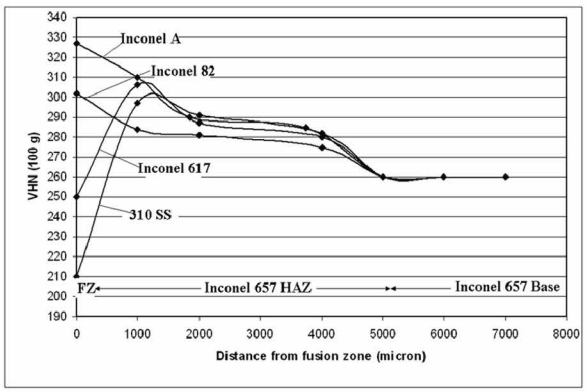

Fig .10. Microhardness measurements versus the distance from weld metal to Inconel 657 base metal.

4- Conclusions

The following conclusions can be drawn from the experimental results:

- The microstructure of Inconel 657 is composed of columnar and equiaxed dendrites. Several second phases are observed in the interdentritic regions.
- The unmixed, the partially–melted, and the heat-affected zones form for both sides of the joints. Inconel 657 base metal shows UZ and PMZ, but no significant PMZ can be observed in the 310 SS base metal.
- Average heat input to the weld puddle governs the average size and structure of the HAZ and UZ in the two dissimilar base metals.
- Precipitation occurs in the heat-affected zone of Inconel 657. Hardness also increases from the weld metal to the HAZ for all the welds.
- It was concluded that undesirable regions such as UZ, HAZ, and PMZ have the least average size for Inconel 82 and 310 SS weldments among the weld metals investigated.

References

[1] G. Belloni, G. Caironi, A. Gariboldi, A. Lo Conte, Trans. SMiRT 16, Washington DC, August 2001, Paper 1546.

[2] R. Kacar, O. Baylan, Mater. Design, 25(2004). 317.

[3] W. Y. Lu, M. F. Horstemeyer, J. S. Korellis, R. B. Grishabr, D. Mosher, Theor. Appl. Fract. Mec. 30(1998), 139.

[4] C. A. Huanga, T. H. Wang, C. H. Lee, W. C. Han, Mater. Sci. Eng. A, 398(2005), 275.

[5] R. C. Yin, A. A. Al-Refaie, B. Al-Yami, A. K. Bairamov, Eng. Failu. Analy. 12(2005), 413.

[6] Li. Jian, C. Y. Yuh, M. Farooque, Corr. Sci., 42(2000), 1573.

[7] S. Zhao, X. Xiea, G. D. Smith, Sur. Coat. Tech.185(2004), 178.

[8] J. N. Dupont, S. W. Banovic, A. R. Marder, Weld. J. 82(2003), 125s.

[9] M. Sireesha, V. Shankar, K. Albert Shaju, S. Sundaresan, Mater. Sci. Eng. A, 292(2000), 74.

[10] M. Sireesha, K. Albert Shaju, V. Shankar, S. Sundaresan, J. Nucl. Mater., 279(2000), 65

[11] T-Y. Kuo, H-T. Lee, Mater. Sci. Eng. A, 338(2002), 202.

[12] H. T. Lee, S. L. Jeng, C. H. Yen, T. Y. Kuo, J. Nucl. Mater., 335(2004), 59

[13] M. D. Rowe, P. Crook, G. L. Hoback, Weld. J., 82(2003), 313s.